

TWO-DIMENSIONAL MODELING OF WATER SPRAY COOLING IN SUPERHEATED STEAM

by

Vahid EBRAHIMIAN and Mofid GORJI-BANDPY

Original scientific paper

UDC: 532.529:66.011

BIBLID: 0354-9836, 12 (2008), 1, 79-88

DOI: 10.2289/TSCI0802079E

Spray cooling of the superheated steam occurs with the interaction of many complex physical processes, such as initial droplet formation, collision, coalescence, secondary break up, evaporation, turbulence generation, and modulation, as well as turbulent mixing, heat, mass and momentum transfer in a highly non-uniform two-phase environment. While it is extremely difficult to systematically study particular effects in this complex interaction in a well defined physical experiment, the interaction is well suited for numerical studies based on advanced detailed models of all the processes involved. This paper presents results of such a numerical experiment. Cooling of the superheated steam can be applied in order to decrease the temperature of superheated steam in power plants. By spraying the cooling water into the superheated steam, the temperature of the superheated steam can be controlled.

In this work, water spray cooling was modeled to investigate the influences of the droplet size, injected velocity, the pressure and velocity of the superheated steam on the evaporation of the cooling water. The results show that by increasing the diameter of the droplets, the pressure and velocity of the superheated steam, the amount of evaporation of cooling water increases.

Key words: cooling water, spray formation, break up model, evaporation, two phase flow, turbulence

Introduction

The majority of computational spray models employ the particle-source-in-cell method [1] or the discrete droplet model (DDM) [2]. The DDM has been employed for a wide range of spray simulations, particularly fuel sprays in engines [3-7]. The DDM involves solving the equations of motion for a turbulent carrier gas in an Eulerian scheme, and integrating Lagrangian equations of motion for liquid droplets along with true pass line. These two calculation schemes, and therefore the two phases, are then coupled through source terms in the transport equations. The major advantages of this over a purely Eulerian scheme are the ability to efficiently discretise the liquid phase into groups of identical droplets, and the fact that the equations for the dispersed liquid phase are more naturally written down in a Lagrangian manner. Modeling of non-stationary turbulent spray formation and evaporation is of practical importance not only for desuperheaters but also for many other technological applications, including transient processes in diesel engines, gas turbine, rocket combustors, and industrial burners, as well as for explosion and detonation studies. Due to the complexity of the processes involved, very few data exist in this domain and thus detailed numerical studies based on advanced models

of the elementary processes are of current interest. The detailed spray evaporation models from the literature [8, 9] use very crude reaction models and thus are unable to reproduce the very complex injection and evaporation behavior of water. Some recent literatures [10-13] have used the spray cooling in practical applications. In this work, $k-\varepsilon$ model is used for turbulence to remove the limitations of current approaches. Simple axi-symmetric spray geometry is used to reproduce the basic features of future direct injection and to model the spray vaporization in superheated flow.

The model

In this work, the spray evaporation in a channel with determined dimensions and properties is modeled. According to fig. 1, superheated steam with the determined velocity, pressure and temperature passes through the channel and cooling water is injected into the superheated steam to control the temperature of the superheated steam. The Lagrangian-Eulerian formulation is

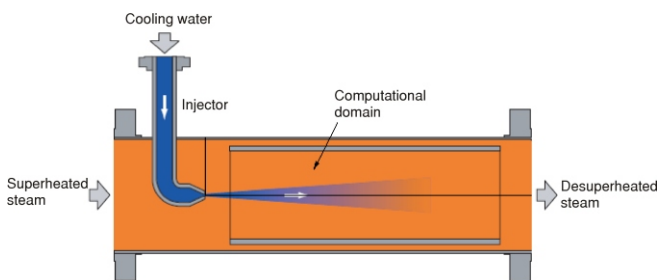


Figure 1. Axial injection spray desuperheater
(color image see on our web site)

treatment is employed to groups of droplets in the so-called “stochastic particle method”, in which a finite number of particles is used to represent the entire spray [14, 15]. In this work, axi-symmetry is assumed and the calculations are carried out only up to the time of injection in order to reduce the computational work.

Droplet phase

The interaction of a droplet with the surrounding gas is illustrated in fig. 2.

A spray can be divided into two or three regions: (a) dilute spray region, (b) dense spray region, and (c) churn flow region. The last is sometimes omitted.

The equations for a single droplet in the dilute spray region read:

– Droplet position

$$\frac{dx_d}{dt} = u_d \quad (1)$$

$$\frac{dr_d}{dt} = v_d \quad (2)$$

– Droplet momentum

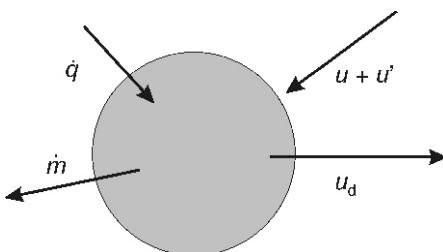


Figure 2. Droplet exchanging momentum, mass, and energy with the surrounding gas

$$\frac{du_d}{dt} = k_d (u - u_d) \frac{1}{\rho_d} \frac{dp}{dx} \quad (3)$$

$$\frac{dv_d}{dt} = k_d (v - v_d) \frac{1}{\rho_d} \frac{dp}{dx} \quad (4)$$

– Droplet mass

$$\frac{dm_d}{dt} = \pi D_d DP_t \ln \frac{p_t}{p_{vs}} \frac{Sh}{RT} \quad (5)$$

– Droplet enthalpy

$$m_d \frac{dh_d}{dt} = \pi D_d k (T - T_d) f(Z) Nu h_v \frac{dm_d}{dt} \quad (6)$$

where, $k_d = (3/4)C_d (\rho/\rho_d)(1/D_d)|\vec{V}_{rel}|$ and $|\vec{V}_{rel}|$ is the relative velocity between gas and liquid phases, $|\vec{V}_{rel}| = \{[\bar{u} - u_d]^2 + [(\bar{v} - v_d)]^2\}^{1/2}$. $f(Z)$ is the correction factor for the effect of mass transfer on the heat transfer coefficient, as given by El Wakil *et al.* [16]. In eqs. (5) and (6), the Sh and Nu are the Sherwood and Nusselt number, respectively, and are defined as: $Sh = 2.0 + 0.6 Re^{0.5} Sc^{0.33}$ and $Nu = 2.0 + 0.6 Re^{0.5} Pr^{0.33}$, where Re, Sc, and Pr are Reynolds, Schmidt and Prandtl number, respectively.

Spray formation

For the spray formation and evaporation, the model proposed by Reitz and Diwakar [17] and Reitz [8] was used with some modifications to improve the droplet break up and droplet collision mechanism for high evaporation rates.

The model was adopted because it removes the need to specify the initial droplet size distribution at the nozzle, which is always a serious problem.

Atomization model

The atomization model tested is Johns and Gosman model [7], including some modifications to improve its performance for high temperature and pressure cases.

Break up model

The Reitz and Diwakar model, in contrast to Huh and Gosman model [18], in which the spray angle is predicted, assumes that this angle is known and given as input. The model uses the concept that atomization of the injected liquid and the subsequent break up of drops are indistinguishable in a dense spray. The model is based on the correlations given by Nicholls [19], in which two regimes are considered:

– bag break up, when the Weber number is:

$$We = \frac{\rho_{gas} w^2 D_d}{2\sigma} \geq 6 \quad (7)$$

– stripping break up, when the ratio:

$$\frac{We}{\sqrt{Re}} \geq 5 \quad (8)$$

In the stripping model, the droplet size changes continuously. In this study, stripping break up model is used.

Collision model

Droplet collision is modeled by the model offered by O'Rourke [20].

Gas phase

The analysis of the gas phase involves solving equations for mass, momentum, and energy. Included is also the k - ε model for the gas phase turbulence. In addition to the conventional single-phase flow analysis, a droplet phase source term must be added ($S_{\phi d}$); for dense sprays, one must also consider effects of void fraction (θ) on the governing equations.

The governing equations for the gas phase can be expressed as one general equation:

$$\frac{\partial}{\partial t}(\rho\theta U\phi) - \frac{\partial}{\partial x}(\rho\theta U\phi) - \frac{1}{r} \frac{\partial}{\partial r}(r\rho\theta V\phi) + \frac{\partial}{\partial x} \Gamma\theta \frac{\partial \phi}{\partial x} - \frac{1}{r} \frac{\partial}{\partial r} r\Gamma\theta \frac{\partial \phi}{\partial r} = \theta S_{\phi} + S_{\phi d} \quad (9)$$

where ϕ can be: density ρ , axial velocity U , radial velocity V , turbulence kinetic energy k , dissipation rate ε , enthalpy h , and species mass concentration Y_i .

The temperature (T) is calculated from the definition of the mixture enthalpy:

$$h(T) = \sum_{i=1}^N \frac{Y_i h_i(T)}{M_i} \quad (10)$$

where M_i is the molecular weight for species i .

The source terms and Γ are given in tabs. 1 and 2 where, in addition to the already defined quantities, $\bar{\omega}_i$ is the chemical reaction rate of species i .

Standard values of $\mu_t = C_{\mu} \rho k^2 / \varepsilon$, $C_{\mu} = 0.09$, $C_{\varepsilon 1} = 1.44$, $C_{\varepsilon 2} = 1.92$, $\sigma_{\rho} = \sigma_Y = 1.0$, $\sigma_k = 1.0$, $\sigma_{\varepsilon} = k^2 / C_{\mu}^{1/2} (C_{\varepsilon 2} - C_{\varepsilon 1})$ [21], and $\sigma_h = 0.9$ were used in the modeling.

Table 1. Source terms S_{ϕ}

ϕ	Γ	S_{ϕ}
1	0	-
U	μ	$\frac{\partial p}{\partial x} - \frac{\partial}{\partial x} \mu \frac{\partial U}{\partial x} - \frac{1}{r} \frac{\partial}{\partial r} r\mu \frac{\partial V}{\partial x} - \frac{2}{3} \frac{\partial}{\partial x} (\mu U \rho k)$
V	μ	$\frac{\partial p}{\partial r} - \frac{\partial}{\partial x} \mu \frac{\partial U}{\partial r} - \frac{1}{r} \frac{\partial}{\partial r} r\mu \frac{\partial V}{\partial r} - 2\mu \frac{V}{r^2} - \frac{2}{3} \frac{\partial}{\partial r} (\mu U \rho k)$
k	μ/σ_k	$G - \rho\varepsilon$
ε	μ/σ_{ε}	$\frac{\varepsilon}{k} (C_{\varepsilon 1} G - C_{\varepsilon 2} \rho\varepsilon)$
h	μ/σ_h	$\frac{\partial p}{\partial t} - \bar{\omega}_h$
Y_{water}	μ/σ_Y	$\rho \bar{\omega}_{\text{water}}$
Y_i	m/σ_Y	$\rho \bar{\omega}_i$

where

$$G = \mu_t \left[2 \frac{\partial U}{\partial x} \frac{\partial V}{\partial r} - \frac{V}{r} \left(\frac{\partial U}{\partial r} - \frac{\partial V}{\partial x} \right)^2 \right] - \frac{2}{3} (\mu_t U - \rho k)$$

and $\mu = \mu_{mol} + \mu_t N_p$ is the number of parcels in fluid element δV , and $N_{d,p}$ is the number of droplets such as a parcel represents.

Details of numerical study

The simulation of the gas phase involves solving transient Eulerian conservation equations for mass, species, momentum, energy, turbulent kinetic energy, and the state equation. In addition to conventional single phase flow analysis, a droplet source term is added to conservation equations representing the exchange of mass, momentum, and enthalpy between the gas and the drops. For dense spray, the void fraction effect is also included in the equations. Droplet motion, break up, collisions, evaporation, and turbulent diffusion are considered. Open space with a side wall where the injection occurs is used as the computational domain. The initial and boundary conditions are as follows. The gas is moving initially with a constant velocity. All gas properties are initially assumed to be uniform. For the gas phase, a control volume formulation is used and PISO (pressure implicit with splitting of operators) algorithm applied, fig. 3. For the liquid phase, Euler integration is used with explicit position, semi-implicit mass and energy and implicit momentum integration scheme. In this work, axi-symetry is assumed and the calculations are carried out only up to the time of injection in order to reduce the computational work. The temperature of the upper wall is constant. The velocity, pressure, and temperature of inflow wall are determined. For the outflow wall, the temperature will be obtained and staggered grid is used. All the governing equations were discretized by numerical finite volume method.

Table 2. Source terms $S_{\phi d}$

ϕ	Γ	$S_{\phi d} \delta V$
1	0	$N_p N_{d,p} \frac{d}{dt} (m_d)_p$
U	μ	$N_p N_{d,p} \frac{d}{dt} (m_d U_d)_p$
V	μ	$N_p N_{d,p} \frac{d}{dt} (m_d V_d)_p$
ε	μ/σ_ε	$C_\infty \frac{\varepsilon}{k} S_{kd}$
h	μ/σ_h	$N_p N_{d,p} \frac{d}{dt} (m_d h_d)_p$
Y_{water}	μ/σ_Y	$N_p N_{d,p} \frac{d}{dt} (m_d)_p$
Y_i	m/σ_Y	—

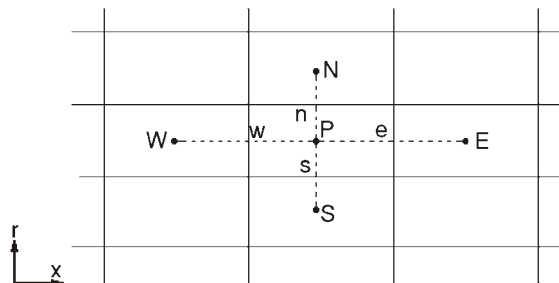


Figure 3. Computational domain

Results and discussion

The case studied involves water jet injected into superheated steam at 550 °C and 150 bar at a velocity of 50 m/s (water pressure in front of the nozzle is 220 bar) through nozzle 0.9 mm in di-

ameter. The computational grid used in the simulation is shown in fig. 4. According to fig. 1, nozzle is located at the first grid.

Figure 5 represents the effect of time step on the total mass of evaporated water (milligram).

According to this figure, by decreasing the time step, the amount of evaporation of water increases. In this work, time step of $6.94 \cdot 10^{-6}$ s is used to obtain the results with a good accuracy and lower computational time consuming.

Controlling the temperature of the superheated steam is significant downstream of the superheaters in the steam boilers of steam power plants. The water evaporated causes the temperature of the superheated steam within the spray to be low.

Figure 6 shows the effect of superheated steam on total mass of evaporated water. According to this figure, by increasing the pressure of the superheated steam (PTRAP), the amount of evaporation of water increases.

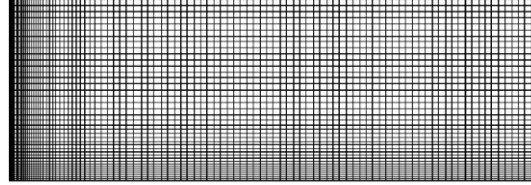


Figure 4. Computational grid 40×100

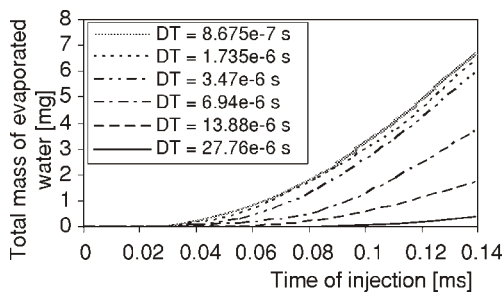


Figure 5. Effects of time step (DT) on the evaporation rate of water cooling spray

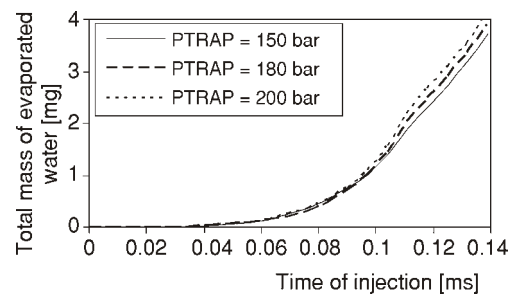


Figure 6. Total mass of evaporated water as a function of time

$P_{inj} = 220 \text{ bar}$, $D_{nozzle} = 0.9 \text{ mm}$, $T_{water} = 300 \text{ K}$, $U_{steam} = 50 \text{ m/s}$

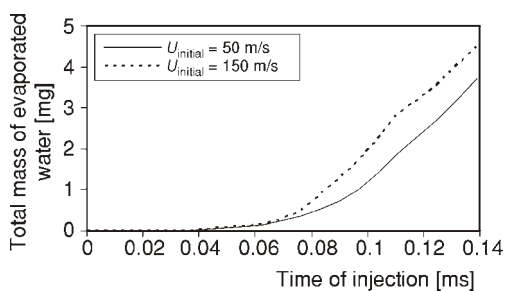


Figure 7. Total mass of evaporated water as a function of time

$P_{inj} = 220 \text{ bar}$, $D_{nozzle} = 0.9 \text{ mm}$, $T_{water} = 30 \text{ K}$

total mass of evaporated water increases by increasing the droplet diameter but it is lower than when break up model is into account.

The differences between the two states; no break up and break up is into account, are shown in fig. 10.

In fig. 7, the effect of velocity on total mass of evaporated water is shown. According to this figure, the amount of evaporation of water increases by increasing the velocity of the superheated steam.

In fig. 8, the effect of droplets on the amount of evaporation of water is shown. According to this figure, by decreasing the droplet diameter (D_{31}), total mass of evaporated water increases.

In fig. 9, the effect of droplets when no break up is into account, on the amount of evaporation of water is shown. According to this figure, total mass of evaporated water increases by increasing the droplet diameter but it is lower than when break up model is into account.

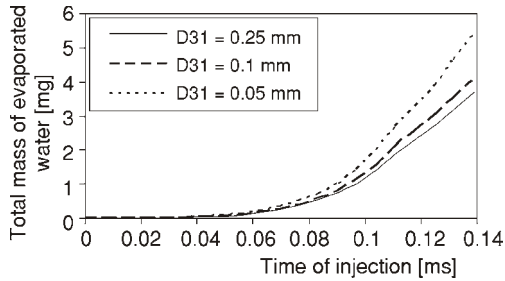


Figure 8. Total mass of evaporated water as a function of time
 $P_{inj} = 220$ bar, $D_{nozzle} = 0.9$ mm, $T_{water} = 300$ K, $U_{steam} = 50$ m/s

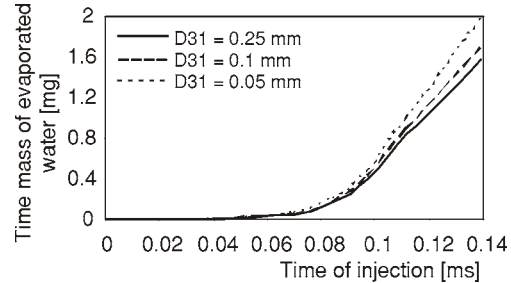


Figure 9. Total mass of evaporated water as a function of time
 $P_{inj} = 220$ bar, $D_{nozzle} = 0.9$ mm, $T_{water} = 300$ K, $U_{steam} = 50$ m/s

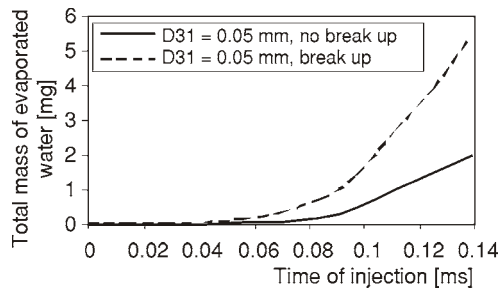


Figure 10. Total mass of evaporated water as a function of time (break up and no break up is into account)
 $P_{inj} = 220$ bar, $D_{nozzle} = 0.9$ mm, $T_{water} = 300$ K, $U_{steam} = 50$ m/s

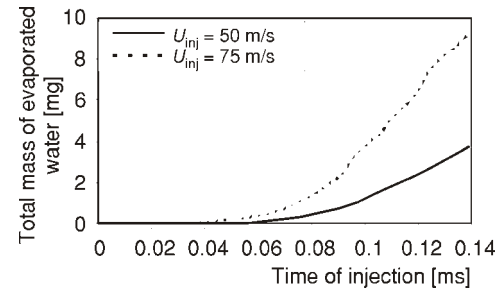


Figure 11. Total mass of evaporated water as a function of time
 $P_{inj} = 220$ bar, $D_{nozzle} = 0.9$ mm, $T_{water} = 300$ K, $U_{steam} = 50$ m/s

In fig. 11, the effect of injected velocity on the total mass of evaporated water is shown. According to this figure, by increasing the injected velocity, the amount of evaporation of water increases.

In fig. 12, velocity vectors for the channel are shown. The effect of turbulence and injection time in the flow field can be seen in this figure.

The effects of injection time on turbulent kinetic energy are shown in fig. 13. By increasing the injection time, turbulent kinetic energy increases. According to this figure, the amount of turbulence is higher near the nozzle, where the concentration of droplets is higher than other places.

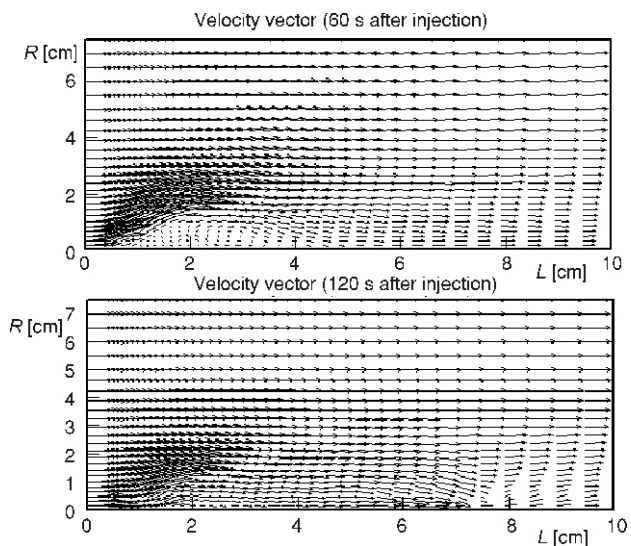


Figure 12. Velocity vectors for different injection times

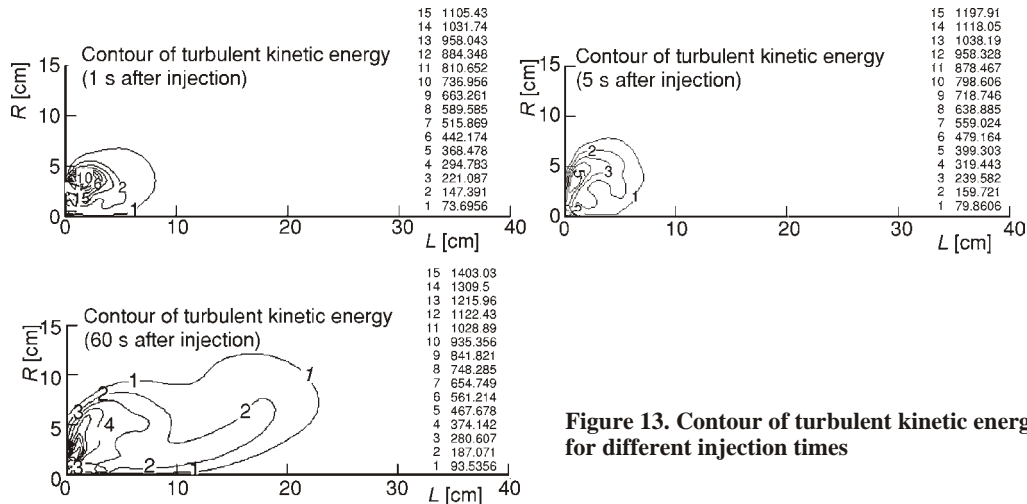


Figure 13. Contour of turbulent kinetic energy for different injection times

The effects of injection time on water vapor mass fraction (WVMF) are shown in fig. 14. The maximum of WVMF is 1, where there is just vapor. By increasing the injection time, WVMF increases. According to this figure, WVMF is higher near the nozzle, where the concentration of droplets is higher than in the other parts of the flow domain.

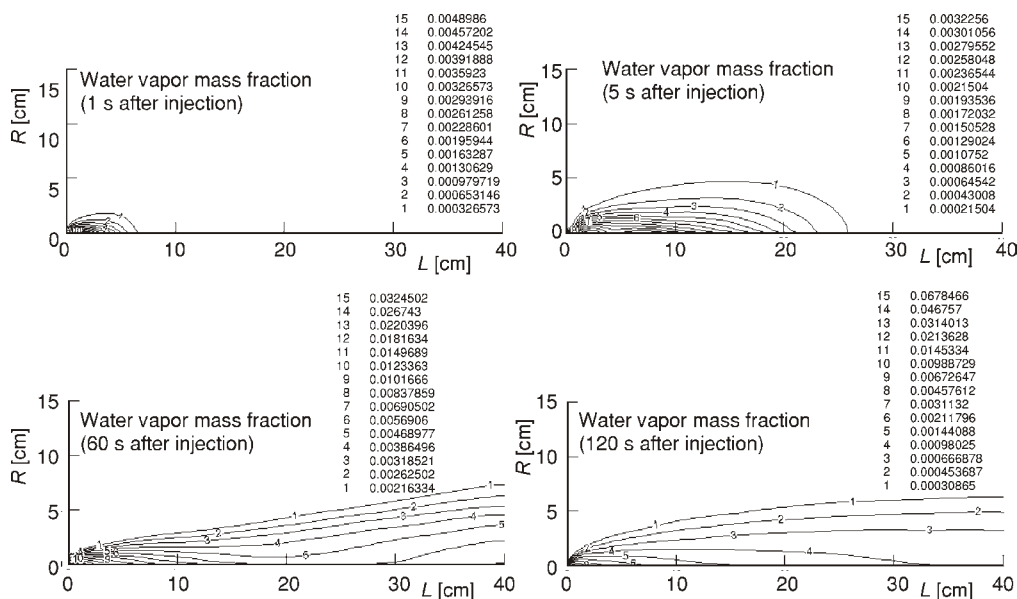


Figure 14. Contour of water vapor mass fraction for different injection times

Conclusions

In order to decrease the temperature of superheated steam in power plants, cooling of the superheated steam can be applied. In this numerical study, water spray cooling was modeled to investigate the influences of the diameter of the droplets, the pressure and velocity of the superheated steam on the evaporation of the cooling water.

- [2] Ducowicz, J. K., A Particle-Fluid Numerical Model for Liquid Sprays, *J. Comp. Phys.*, 35 (1980), 2, pp. 229-253
- [3] Gosmann, A. D., Johns, R. J. R., Computer Analysis of Fuel-Air Mixing in Direct-Injection Engines, SAE paper 800091, 1980
- [4] Reitz, R. D., Modeling Atomization Processes in High Pressure Vaporizing Sprays, *Atomization and Spray Technology*, 3 (1987), 4, pp. 309-337
- [5] Amsden, A. A., O'Rourke, P. J., Butler, T. D., KIVA-II: A Computer Program for Chemically Reactive Flows with Sprays, Technical Report LA-11560-MS, Los Alamos National Laboratory, 1989
- [6] Watkins, A.P., Three-Dimensional Modeling of Gas Flow and Sprays in Diesel Engines, Computer Simulation for Fluid-Flow, Heat and Mass Transfer and Combustion in Reciprocating Engines, (Ed., N.C., Markatos), Hemisphere, Publ. Comp., New York, USA, 1989
- [7] Chen, X. Q., Perreira, J. C. F., Numerical Predictions of Evaporating and Non-Evaporating Sprays under Non-Reactive Conditions, *Atomization and Sprays*, 2 (1992), 4, pp. 427-433
- [8] Kachhwaha, S. S., Dhar, P. L., Kale, S. R., Experimental Studies and Numerical Simulation of Evaporative Cooling of Air with a Water Spray: Part I: Horizontal Parallel Flow, *International Journal of Heat and Mass Transfer*, 41 (1998), 2, pp. 447-464
- [9] Kachhwaha S. S., Dhar P. L., Kale S. R., Experimental Studies and Numerical Simulation of Evaporative Cooling of Air with a Water Spray: Part II: Horizontal Counter Flow, *International Journal of Heat and Mass Transfer*, 41 (1977), 2, pp. 465-474
- [10] Belarbi, R., Ghiaus, C., Allard, F., Modeling of Water Spray Evaporation: Application to Passive Cooling of Buildings, *Solar Energy*, 80 (2006), 12, pp. 1540-1552
- [11] Zima, W., Simulation of Dynamics of a Boiler Steam Superheater with an Attemperator, *Proceeding*, Institution of Mechanical Engineers, Part A, *Journal of Power and Energy*, 220 (2006), A7, pp. 793-801
- [12] Hsieh, S. S., Tien, C. H., R-134a Spray Dynamics and Impingement Cooling in the Non-Boiling Regime, *International Journal of Heat and Mass Transfer*, 50 (2007), 3-4, pp. 502-512
- [13] Yoon, S. S., Kim, H. Y., DesJardin, P. E., Unsteady RANS Modeling of Water-Spray Suppression for Large-Scale Compartment Pool Fires, *Atomization and Sprays*, 17 (2007), 1, pp. 1-45
- [14] Faeth, G. M., Mixing, Transport and Combustion in Sprays, *Prog. Energy Combust. Sci.*, 13 (1987), 4, pp. 293-345
- [15] Faeth, G. M., Evaporation and Combustion of Sprays, *Prog. Energy Combust. Sci.*, 9 (1983), 1-2, pp. 1-76
- [16] El Wakil, M. M., Ueyhara, Q. A., Myers, F. S., A Theoretical Investigation of Heating-Up Period of Injected Fuel Droplets Vaporizing in Air, NACA Report No. TN 3179, 1954
- [17] Reitz, R. D., Diwakar, R., Structure of High-Pressure Fuel Sprays, *SAE Trans.*, Vol. 97, Sect. 5, Paper 870598, pp. 492-509, 1988
- [18] Huh, K. Y., Gosman, A. D., A phenomenological Model of Diesel Spray Atomization, International Conference on Multiphase Flows, Tsukuba, Japan, 1991, Vol. 2, pp. 515-518
- [19] Nicholls, J., Stream and Droplet Break up by Shock Waves, NASA SP-194, 1972
- [20] O'Rourke, P. J., Collective Drop Effects on Vaporizing Liquid Sprays, Los Alamos National Laboratory Report LA-9069-T, 1981
- [21] Rodi, W., Turbulence Models and Their Application in Hydraulics – A State-of-the-Art Review, IAHR, The Netherlands, 1984

Authors' address:

V. Ebrahimian, M. Gorji-Bandpy
Faculty of Mechanical Engineering,
Noushivani Institute of Technology,
P. O. Box 484, Babol, Iran

Corresponding author M. Gorji-Bandpy
E-mail: gorji@nit.ac.ir

Paper submitted: January 17, 2007
Paper revised: December 2, 2007
Paper accepted: December 7, 2007